The Residence Time and Slow Pyrolysis Temperature Effect on Chemical Composition Pyrolysis Gas Product of Durian (*Durio Zibethinus Murr*) Skin

Rizka Wulandari Putri[a,*], Rahmatullah[a], Sri Haryati[a], Budi Santoso [a], Alek A Hadi[b]

[a]Chemical Engineering Department, Engineering Faculty, Sriwijaya University, South Sumatera, Indonesia
[b]Mining Engineering Department, Engineering Faculty, Sriwijaya University, South Sumatera, Indonesia
 rizkawulandariputri@unsri.ac.id

Durian (Durio Ziberthinus Murr) is a commodity fruit in Southeast Asia especially in Malaysia, Thailand and Indonesia. Durian skin contains lignin, cellulose, and hemicellulose and is the potential to be converted into several solid, liquid, and gas products by a slow pyrolysis process. This work strived to observe the effect of residence time and temperature on pyrolysis-gas product composition. Durian skin (DS) in size 4-5 cm was pyrolyzed in a fixed bed pyrolysis reactor with natural zeolite inside at the temperature range of 300 °C - 400 °C for 10 min and 30 min. The yield of pyrolysis gas products and gas product components was determined in this work. The pyrolysis gas product was analyzed using Gas Chromatography (GC) to determine the components of gas such as CO, CH_4 and H_2 along with CO_2 gas. The best performance was achieved at 300 °C for 30 min residence time with gas products 29.8 ng/ul CO_2, 30.89 ng/ul CO, 13.08 ng/ul CH_4 and 8.17 ng/ul H_2. The characteristics of the zeolite used were analyzed by X-ray Diffraction (XRD) to determine the effect of activation and pyrolysis product on the catalyst crystal transformation.

1. Introduction

Durian (*Durrio zubethinus Linn*) is a famous fruit in Southeast Asia, especially in Malaysia, Thailand and Indonesia. People of these countries consume durian flesh (20.92 %) and waste the remaining seeds and skin (79.08 %) (Wahidin et al., 2014). Durian skin (DS), as the wasted part of the fruit, has significant potential to become an alternative fuel. DS mainly contains lignin, cellulose, and hemicellulose. It embodies 50 % - 60 % of high cellulose, 5 % of lignin, and 5 % of low starch (Prabowo, 2009). The DS will become the alternative energy source when its high lignocellulose content undergoes the thermochemical process. The thermochemical process is a conversion method by thermal for converting biomass into fuel or chemical products (McKendry, 2002). During thermochemical conversion (combustion, pyrolysis, and gasification), biomass turns into solid, liquid, and gaseous forms, which can be synthesized through chemical processes or used directly (Basu, 2010). During the thermochemical process, the three main components of DS will undergo a decomposition process at different temperatures. Lignin, hemicellulose, and cellulose will decompose at 160 - 900 °C, 220-315 °C, and 315 - 400 °C (Yang et al., 2010).

One of the most effective lignocellulose decomposition processes is pyrolysis. Pyrolysis is part of the thermochemical method in the absence of oxygen. Pyrolysis splits into three categories based on the heating rate and heating temperature; slow, medium, and fast pyrolysis. Slow pyrolysis occurs at low temperatures (300 - 400 °C) with >15 min of heating time and 50 °C/min of heating rate. Then, the medium one happens at a moderate temperature (500 °C) with 200 °C/min of heating rate. Fast pyrolysis exists at high temperatures from 600 – 700 °C with <5 min of heating time and 10 – 1000 °C/min of heating rate (Zeng et al., 2017).

Many researchers have conducted studies on pyrolysis. Kampegowda and Pongchan (2008) investigated the slow pyrolysis on rice straw and produced a charcoal product with 4337 kcal/kg of Low High Value (LHV). Slow pyrolysis of rice straw was examined in a bench-scale fixed bed pyrolysis reactor. Shakita (2021) researched the effect of pyrolysis temperature (300, 400, 500, and 600 °C) and residence time (1, 2, and 3 h) on product yield distribution and energy yield and discovered that the concentration of CO and CO_2 decreased gradually

from 41.81-29.66% and 54.02-38.46%, while H_2 and CH_4 increased from 1.9-19.22% and 2.3-10.54%. Suhendi et al. (2021) studied the influence of natural zeolite on palm oil shell pyrolysis at 500 °C. The employment of activated natural zeolite catalysts increased CO, CH_4, and H_2 gas levels by decreasing CO_2 with a gas yield of around 46%, which was better than the one without zeolite (44 %) (Suhendi et al., 2021).

The present study focuses on the natural zeolite application as the catalyst to enhance pyrolysis performances at low temperatures. Zeolite is an alumina silicate crystal with a microporous structure and utilized as a catalyst with particular characteristics in its pore size, pore distribution, and ion exchange capabilities. Zeolite catalyst brings efficiencies in the slow pyrolysis process and allows reactions to emerging more quickly or at lower temperatures due to change it triggers in reagents (Oyeleke et al., 2021).

In this study, slow pyrolysis of DS was processed at 300 - 400 °C with natural zeolite as the catalyst in 10 min and 30 min residence time. The yield of the pyrolysis product was measured, and the gas product components were analyzed to show the best performance of zeolite in the slow pyrolysis process

2. Methods

This research transpired in several stages of the procedure, including raw material preparation and the slow pyrolysis process. The yield of gas product was calculated, and the gas product components were analyzed using gas chromatography (GC). The zeolite characterization during pre-activation, post-activation and after the pyrolysis reaction was analyzed to determine the effect of activation and pyrolysis reaction on the size and intensity of zeolite crystals.

2.1 Raw material preparation

This research began by preparing the raw material for durian skin (DS) from Prabumulih, South Sumatera. DS was washed with distillate water and reduced to 4-5 cm with a grinder machine. DS was dried in the sun until reached constant weight. The 300 g of dried DS was placed in the pyrolysis reactor.

Table 1 displays the proximate and calorific value analysis results. Those tests were to predict the possibility of DS becoming an alternative fuel. This research calculated the calorific value using bomb calorimeter Model-IKA C2000, placed the sample into the bomb, and chose determination on the operation menu for coal samples or standardization for Benzoic AC ID. As the temperature on the heater stabilized at ± 30 °C, the process proceeded. Table 1 reveals that durian skin is likely alternative fuel due to its high calorific value (15.89 MJ/kg) compared to one in palm oil plants (14.77 Mj/kg) (Satria et al., 2016). (Satria et al, 2016).

Table 1: Proximate analysis and calorific value of DS

Proximate analysis (wt% in dry at room temperature)				Calorific Value (MJ/kg)
Fixed Carbon	Volatile Matter	Ash	Moisture	
10.38	64.04	8.14	10.38	15.89

2.2 Slow pyrolysis process

The 300 g of dried DS went into a fixed bed reactor containing 4 % wt natural zeolite. The zeolite was prepared for activation by calcined at a temperature of 450 °C for 4 h to open the pores and active site of zeolite (Kusuma et al., 2013). Slow pyrolysis was carried out at a temperature of 300 – 400 °C with variations in 10 min and 30 min residence time, as stated by Jouhara's statement (2018). The output product proceeded to the holding tank, and the yield of product pyrolysis gas was calculated and sent for gas chromatography analysis.

2.3 Gasification product analysis

The chemical composition analysis of the gas produced from the gasification process of DS was used GC-TCD type variant 4000 with a carbon molecular sieve column (Carboxen1010 PLOT Capillary GC Column) to determine the gas product components. The sample was injected into the GC without an intermediary and using an autosampler with Helium as the carrier gas. Afterwards, the sample evaporated, and the gas passed through the column in a GC oven at 50 °C for 2 min. Based on the percent composition of CO, CH_4 and H_2, the percent yield gas is calculated using Eq (1):

$$\text{Gas Comb} = (Y\,CO + Y\,CH_4 + Y\,H_2) \times 100\ \% \tag{1}$$

where Y CO is the mole fraction of CO; Y CH_4 is the mole fraction of CH_4; and Y H_2 is the mole fraction of H_2 (Sanjaya et al., 2018).

2.4 Characterization of Zeolite

As the catalyst, zeolite characterization occurred in pre-activation, post-activation, and after the pyrolysis process. In this process, the X-ray Diffraction (XRD) type Rigaku Mini Flex analyzed the crystals, and the zeolite characterization determined their morphological form (shape and size). Next, zeolite samples (before activation, after activation, and after pyrolysis) were pulverized into powders and pressed. Then, the powdered zeolite sample was placed in the sample holder and X-rayed with Cu Kα radiation of 1.541 A) at a speed of 3o/second (Intarapong et al., 2013). Identification to determine the crystal size with a certain phase used a modification of the Deybe Scherrer Equation (Monshi et al., 2012) as in Eq (2):

$$D = \frac{k\lambda}{\beta \cos \theta} \tag{2}$$

Where D is Crystal size (nm), k is Crystal form factor (0.9-1), λ is X-ray wavelength (0.15406 nm), β is Value of Full Width at Half Maximum (FWHM) (rad), and θ = Angle of diffraction (degrees).

XRD instruments were to monitor the process of chemical reactions and material synthesis. The specificity of the diffraction pattern of a compound changed if it reacted to other compounds. Changes in the diffraction pattern were the principle of analysis-synthesis process using XRD (Fuentes, et al., 2001). The diffractogram pattern was the series of diffraction peaks with relative intensity varying along a certain 2θ value.

3. Result and discussion

Experimental conditions and procedures like variations in temperature and residence time affected he product yield. The gas composition of the pyrolysis product also indicated different results in each variation of temperature and resident time.

3.1 The effect of temperature on pyrolysis gas component

Thermal decomposition of biomass happens through four stages of pyrolysis, namely drying stages (100 °C), initial stage (100 -300 °C), intermediate stage (>200 °C or 200 – 600 °C), and final stage (300 – 600 °C). The dissimilarity of temperatures at each stage refers to the different decomposition of biomass components (Basu, 2010). During the decomposition process, the lignocellulose structure will release gas. Therefore, when the pyrolysis decomposes various biomass components (such as hemicellulose, cellulose, and lignin), variants of gas components will be released. At temperatures 350 and 400 °C, the gas composition produced is $CO_2>CO>CH_4>H_2$, indicating CO_2 gas is dominant in the cellulose decomposition, and CO was more prominent than CH_4 and H_2 (Quan et al., 2016). On the other hand, the temperature of 300 °C assembles $CO>CO_2>CH_4>H_2$ composition, implying that hemicellulose decomposition occurs at this heat. The effect of temperature variation on the amount of gas product at 10 and 30 min of this study is revealed in the Figure 1 below.
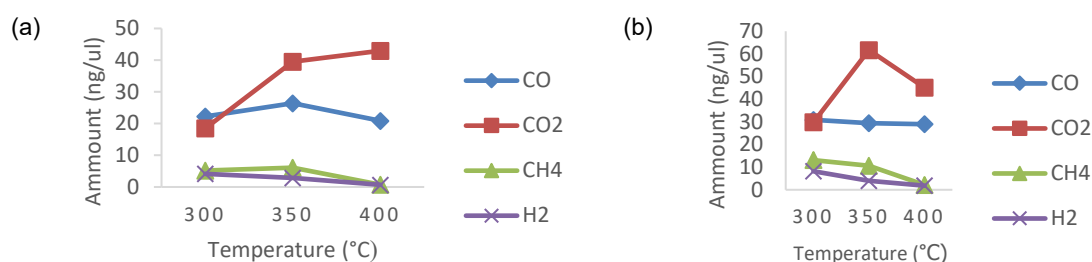

Figure 1: (a) The effect of temperature variation on the amount of gas product at 10 min (b) The effect of temperature variation on the amount of gas product at 30 min

Figure 1 displays the composition of the pyrolysis gas products of this study. The CO_2 gas from the pyrolysis process fluctuates in temperature variation, and CO gas changes insignificantly. As seen in Figure 1b, at 300 °C, the gas composition produced is $CO>CO_2>CH_4>H_2$ with CO, CO_2, CH_4, and H_2 values are 30.89 ng/ul, 29.8 ng/ul, 13 ng/ul, and 8.17 ng/ul. Meanwhile, at temperatures above 315 - 400 °C, the gas composition is $CO_2>CO>CH_4>H_2$ (Figures 1a and 1b). This condition was in line with Yang's (2010) statement mentioning that hemicellulose occurred at the temperature of 220 - 315 °C with the gas component of $CO>CO_2>CH_4>H_2$, and cellulose decomposition occurred at the temperature of 315 - 400 °C with the gas component of $CO_2>CO>CH_4>H_2$.

3.2 The effect of residence time to pyrolysis gas products

From Figure 1b, the best pyrolysis performance in this study was achieved at a temperature of 300 °C and a residence time of 30 min. At these conditions, the lowest CO_2 gas produced was 30.8 ng/ul, and the highest combustible gases CO, CH4 and H2 (29.8 ng/ul, 13.1 ng/ul and 8.18 ng/ul). The result indicated that long residence time and low heating temperature directed gas production increases (Bridgewater, 2012). In Figure 3, the composition if combustible gas was calculated with eq (1) which was the sum of the yields of CO, CH4 and H2 gases. The combustible gases (CO, CH4 and H2) decreased as the temperature increased.
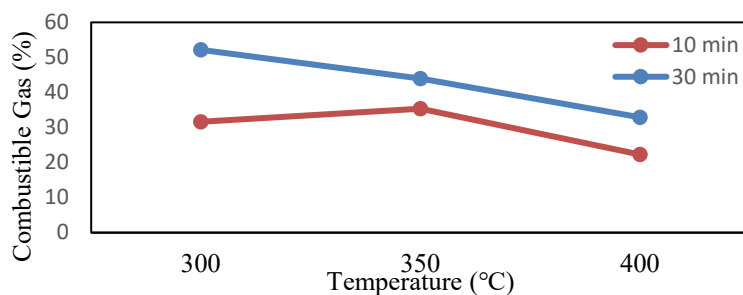

Figure 2. Comparison of combustible gas on residence time 10 min and 30 min

Based on Figure 2, during 10 min of residence time, the temperature of 300 °C produced 31.59 % combustible gas, and the temperature 350 °C increased slightly to 35%. Meanwhile, at a temperature of 400 °C, the combustible gas decreased by 22.27 % because high temperature tended to form majority CO_2 gas. On the other hand , at a residence time of 30 min, the most combustible gas produced at a temperature of 300 °C with a value of 52.15 %. It was supported by Al (2018) stated that for methane and other combustible gas favored low temperatures. In many cases, the syngas was also highly dependent on feedstock used as well as temperature (Jouhara et al., 2018).

3.3 The effect of activation and pyrolysis process on zeolite characteristics

The natural zeolites are low in crystallinity. Therefore an activation is needed to improve the crystal size (Suhendi et al., 2021). The crystal size value (D) was obtained with the Eq (2). The result showed the crystal size of zeolite in the range 144.18 to 156.62 nm. The comparison of the crystal size of the natural zeolite catalyst before activation (BA), after activation (AA), and zeolite after the pyrolysis process (AP) was calculated using the modified Eq (2). The results of the crystal sizes comparison of zeolite shown in Table 2

Table 2. Crystal size of zeolite in variant condition

Sample	Crystal size (nm)
Before activation (BA)	156.62
After activation (AA)	144.18
After pyrolysis (AP)	155.77

Table 2 represented the decrease in crystal size on the zeolite sample before activation, after activation and after pyrolysis. This phenomenon indicated that the activation process in natural zeolite could be reduce the crystal size, where the smaller crystal size provided a larger surface area of natural zeolite and increased the active site (Qiang, et al., 2017).

The results of this study are also translated into a diffractogram pattern. The diffractogram pattern is a series of diffraction peaks with relative intensity varying along a certain 2θ value. The relative intensity of the series of peaks depended on the number of atoms or ions present and their distribution within the unit cell of the material (Chook, et al., 2012). The diffraction peak of zeolite crystals after activation increased compared to pure, inactivated zeolite. The top peak of zeolite after activation was 36.10 ° and then decreased after the pyrolysis reaction to 30.64 °. The before-activation process represented the peaks with the sharp intensity that occurred in the 2Ɵ region of 10.06 °, 22.57 °, 25.98 °, and 28.07 °. On the other hand, the after-activation revealed that increased peaks with sharp intensity occurred in the 2Ɵ region at 19.78 °, 22.61 °, 26.02 °, 27.98 °,and 36.10 °. In the after-pyrolysis process, the intensity peaks of zeolite decreased with sharp intensity occurring in the 2Ɵ region at 10.17 °, 22.60 °, 26.00 °, 28.37 °, and 30.64 ° (See Figure 3)
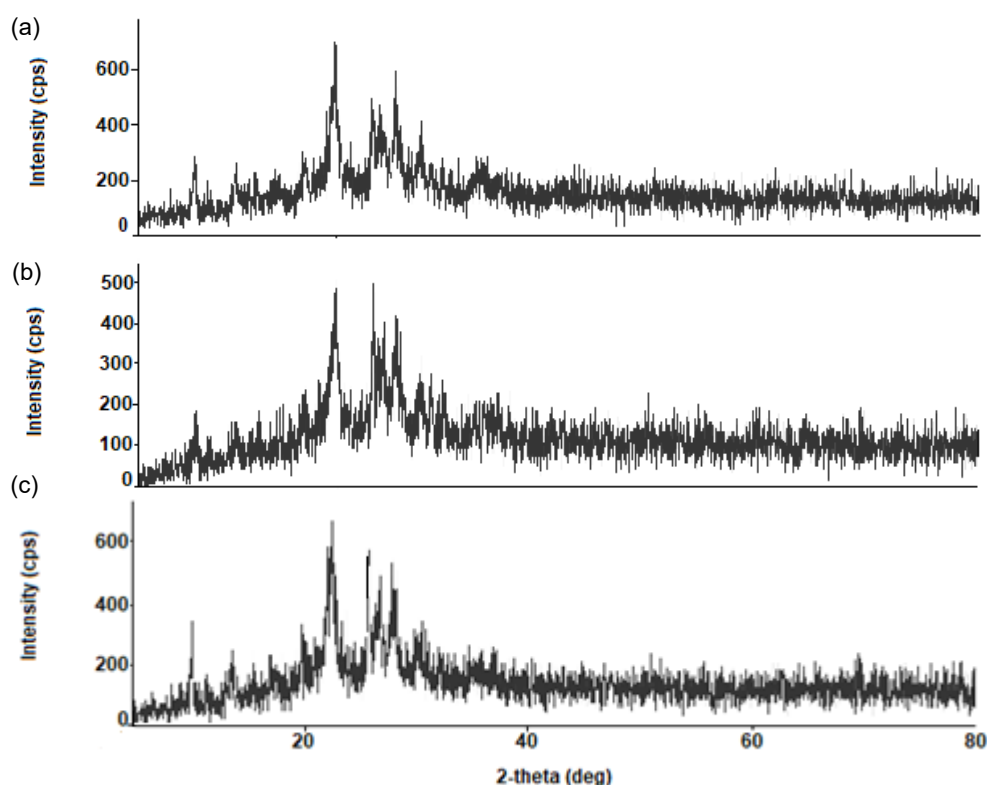
Figure 3. (a) XRD result of zeolite before activation (BA) (b) XRD result of zeolite after activation (AA) (c) XRD result of zeolite after pyrolysis process (AP)

XRD peak positions are identical because chemical compositions, physical properties, and chemical properties are similar. The crystals become smaller with the increase of XRD relative intensity. On the contrary, large crystal has less broadened peaks (Inoue and Izumi, 2013). Based on Figure 3, the BA zeolite has a higher intensity representing a bigger crystal size of about 156.56 nm and causing the smaller surface area of the crystal. The activation process leads to the decrease of intensity from 650 cps to 500 cps. Broader crystal surface area is more effective in expanding the active site due to the crystal size reduction to 144.18 nm. The pyrolysis process causes the intensity of AA zeolite to increase from 500 cps to 600 cps. This conditions implied damage to the carbon composition, which reduced the crystal surface area when the crystal size expanded to 155.77 nm. In other words, the carbon composition changes on the degree of activation (Lee et al., 2021).

4. Conclusions

The slow pyrolysis process was conducted at 300 - 400 °C and 10 and 30 min of residence time. The best performance with the maximum combustible gas product occurred at a temperature of 300 °C and a residence time of 30 min. The gas products were 29.8 ng/ul CO_2, 30.89 ng/ul CO, 13.08 ng/ul CH_4 and 8.17 ng/ul H_2. The results conclude that a long residence time and low heating temperature increased gas production with 52.15 % of gas combustible that revealed similar results to the previous related research of Al (2018). The zeolite activation process is able to maximize the surface area (contact area) due to the decrease of crystal size during the activation process about 144.18 nm.

References

Al A. S., 2018, Comparison of slow and fast pyrolysis for converting biomass into fuel, Renewable Energy, 124,197- 201.

Basu P., 2010, Biomass gasification and pyrolysis: practical design and theory, Elsevier, London, United Kingdom.

Chook S. W., Chin H. C., Sarani Z., Mohd K. A., Kah L. C., Nay M. H., Hui M. N., Hong N. L., Rahman J., Raha M. F. R. A. R., 2012, Antibacterial performance of Ag nanoparticlesand AgGO nanocomposites prepared via

rapidmicrowave-assisted synthesis method, Research Letters, Universiti Kebangsaan Malaysia, Selangor, Malaysia.

Fuentes F. M., Figueiredo F. M. B., Marques J. I., Franco., 2001, Influence of microstructure on the electrical properties of NASICON materials, Solid State Ionics, 140, 173–179.

Ilmawati W. O. S., Jahiding M., Musnina W. O. S., 2017, Pyrolysis temperature effect on volume and chemical composition of liquid volatile matter of durian shell, The 1st IBSC Conference: Towards the Extended Use of Basic Science for Enhancing Health, Environment, Energy and Biotechnology, 26th- 27th September, Jember, Indonesia, 273 – 275.

Inoue M., Izumi H., 2013, The relationship between crystal morphology and XRD peak intensity on $CaSO_4 \cdot 2H_2O$, Journal of Crystal Growth, 380, 169 –175.

Intarapong P., Iangthanarat S., Phanthong P., Leungnaruemitchai A., Jai-In, S., 2013, Activity an basic properties of KOH/mordenite for transesterification of palm oil. Journal of Energy Chemistry, 22, 690 –700.

Jouhara H., Daren A., Inge V. D. B., Evina K., Stefan S., Nik S., 2018, Pyrolysis of domestic based feedstock at temperatures up to 300 C, Thermal Science and Engineering Progress, 117 –143.

Kampegowda M.R., Pongchan C., 2008, Slow pyrolysis for rural small biomass energy by joint project developmentos of Brazil and Thailand, Research Letters, Asian University, Chonburi, Thailand.

Kusuma R. I., Hadinoto J. P., Ayucitra A., Soetaredjo F. E., Ismadji S., 2013, Natural zeolite from pacitan Indonesia, as catalyst support for transesterification of palm oil, , Applied Clay Science, 74, 121–126.

Lee S. M., Sang-Hye L., Jae-Seung R., 2021, Analysis of activation process of carbon black based on structural parameters obtained by XRD analysis, Crystals, 11, 1–11.

Mckendry P., 2002, Energy production from biomass: overview of biomass, Bioresource Technology, 83, 37– 46.

Monshi A., Foroughi M. R., Monshi M. R., 2012, Modified scherrer equation to estimate more accurately nanocrystallite size using XRD, World Journal of Nano Science and Engineering, 2, 154–160.

Oyeleke O. O., Olayinka S. O., Damola S. A., 2021, Catalytic pyrolysis in waste to energy recovery applications: a review, 5th International Conferences on Engineering for Sustainable World, IOP Conference Series: Material Science and Engineering, 10th – 12th November, Ota, Nigeria, 1 – 16.

Prabowo R., 2009, Utilization of durian skin waste as a briquette product in the Gunung Pati sub-district, Semarang district, Journal of Mediagro II, 5(1), 52 – 57.

Quan C., Gao N., Song Q., 2016., Pyrolysis of biomass components in a TGA and a fixed-bed reactor: thermochemical behaviors, kinetics, and product characterization, Journal Analysis and Application of Pyrolysis, 121, 84 – 92.

Lee S. M., Sang-Hye L., Jae-Seung R., 2021, Analysis of activation process of carbon black based on structural parameters obtained by XRD analysis, Crystals, 11, 1-11.

Sanjaya D., Notosudjono D., Fiddiansyah D. B., 2018, Planning for gasification from palm oil waste as alternative energy at PTPN VIII Cikasungka Bogor, Student Online Journal in Electrical Engineering, 1(1), 1 – 14.

Sakhiya A. K., Paramjeet B., Shivangi P., Virendra K. V., Priyanka K., 2020, Effect of process parameters on slow pyrolysis of rice straw: product yield and energy analysis, The International Conference on Utilities and Exhibition ICUE 2020 on Energy, Environment and Climate Change, 20th- 22th October, Pataya, Thailand, 1– 9.

Satria B. Y., Roy F. A. P., Hamid A. A., Ari S. S., 2016, Characteristics biomass for raw materials pyrolysis reactor, Proceeding National Seminar of Chemical Engineering, 17 March, Yogyakarta, Indonesia, 1 – 4.

Wahidin N., Nurfa A., Martana T., 2014, Synthesis preliminary studies durian peel biobriquette as an alternative fuel, Energy Procedia, 47, 295 – 302

Yang H., Yan R., Chen H., Lee D. H., Zheng C., 2010, Characteristics of hemicellulose, cellulose and lignin pyrolysis, Fuel, 86, 1781-1788.

Zeng K., Gauthier D., Minh D. P., Weiss H. E., Nzihou A., Flamant G., 2017, Characterization of solar fuels obtained from beech wood solar pyrolysis, Fuel, 188, 285-293.